AD-A163 902 THE ANALYSIS OF NEAR-EARTH SATELLITE ASTROMETRIC DATA AT THE ETS(U) MASSACHUSETTS INST OF TECH LEXINGTON LINCOLN LAB L G TAFF 12 DEC 85 ETS-76 ESD-TR-85-263 1/1

UNCLASSIFIED F19628-85-C-0002 F/G 22/3 NL

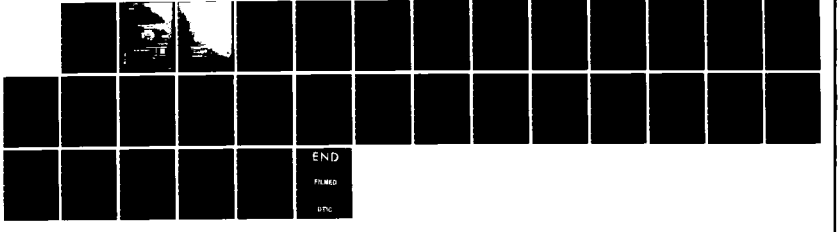

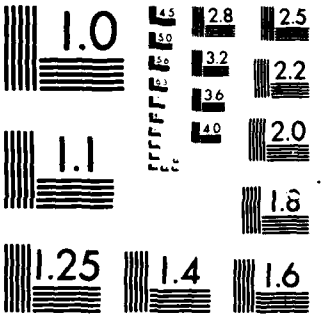

MICROCOPY RESOLUTION TEST CHART
NATIONAL BUREAU OF STANDARDS 1963 A

MASSACHUSETTS INSTITUTE OF TECHNOLOGY
LINCOLN LABORATORY

THE ANALYSIS OF NEAR-EARTH SATELLITE ASTROMETRIC DATA AT THE ETS

L.G. TAFF

Group 94

PROJECT REPORT ETS-76

12 DECEMBER 1985

Approved for public release; distribution unlimited.

LEXINGTON MASSACHUSETTS

ABSTRACT

The activites at the ETS have expanded from observations of deep-space artificial satellites during the dark hours to observations of near-Earth satellites near noon. Not only do these varying tasks require different video cameras and associated equipment, they can benefit from a tailored analysis of the resulting astrometric data. In particular, the observation of near-Earth artificial satellites very near the astronomical zenith has become a frequent mode of operation. For some of these satellites a parallax can be discerned when both ETS telescopes are used. For others, their nearly circular orbit coupled with a zenith passage suffices to fix their element set. This Project Report details both types of analysis.

QUALITY INSPECTED 3

Accesion For	
NTIS CRA&I	☑
DTIC TAB	☐
Unannounced	☐
Justification	
By	
Distribution /	
Availability Codes	
Dist	Avail and / or Special
A-1	

CONTENTS

I. INTRODUCTION

Certain artificial satellites are best illuminated at twilight. The reason is they are so close to the Earth that were it darker they would be eclipsed. Clearly were it brighter than twilight, their phase angle would be larger and the sky background would be very bright. A consequence of these considerations is that they are most easily observed near the zenith. A result of their closeness to the Earth is increased atmospheric drag. Therefore, whether by design or owing to natural forces, their orbits are nearly circular. Hence, there are only four meaningful entries in their orbital element set, not six.

The bulk of this Report is concerned with two different methods of obtaining these four quantities as a result of observing the nearly zenithal passage of an artificial satellite in a nearly circular orbit. Two cases are presented. In the first instance, a satellite beyond about 1000 km will move slowly enough across the small field of view of the ETS telescopes to allow for a good deduction of its angular velocity. This plus the position and the relevant celestial mechanics uniquely determines the element set. In the second case the satellite is much closer and moves too fast to reliably determine its speed. However, its very closeness means that it has a measurable parallax. The measurement of the parallax, the slope of the

streaks, and the position also uniquely defines the element set.

This Project Report discusses both of these cases in depth. The principal aspect of the analysis missing is an estimation of the errors involved for we usually observe an object slightly off the zenith, whose orbit is not truly circular, and so on. As observing needs demand, more sophistication will be introduced.

II. POSITION PLUS ANGULAR VELOCITY

A. Data Acquisition

From a videotape of the passage of a near-Earth satellite played back in very slow motion one can clearly see the progression of the head of the streak. If the recorder has a stop frame mode, then individual frames (and fields; the 1/30 of a second video frame consists of two 1/60 of a second interleaved video fields) can be viewed. The addition of a device for measuring location on the videotape and a frame counter complete the data acquisition hardware (see Figs. 1 and 2).

With such a setup (Fig. 2) one can make a progression of pairs of (say) rectangular coordinate measures of the head of the streak. A simple method of treating the data that smooths out non-linearities in the camera target, stretching of the videotape, and so on, is to difference them pairwise. Division by the appropriate number of frames, multiplication by 30, and then multiplication by the plate scale gives the velocity in arc seconds per second of time. Averaging a series of such pairwise-differenced velocities across the field of view provides the angular velocity data for analysis.

It is useful to be able to determine the orbital inclination from the slope of the streak. To this end the pairs of points are fit, via the method of least squares, to a straight line. The last piece of information needed is the position and we know

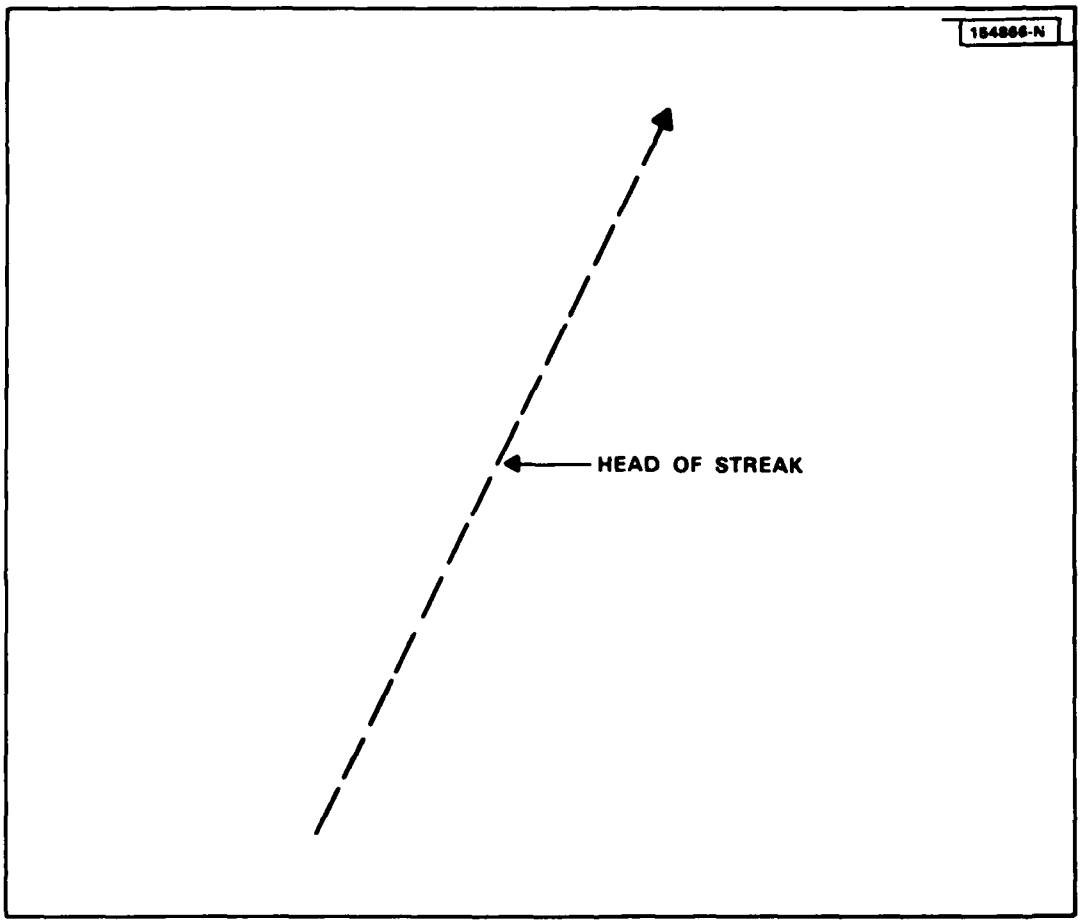

Figure 1. Schematic representation of a succession of overlaid video frames showing the progressive movement of the head of a satellite's streak.

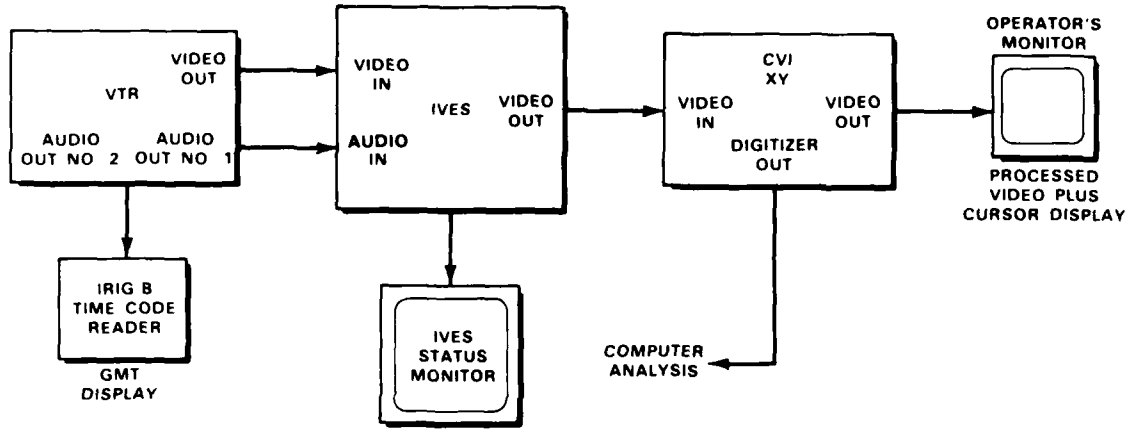

Figure 2. Block diagram of hardware used to measure an approximation of focal plane coordinates from videotapes.

that; it is at the zenith at the time of observation.

B. Celestial Mechanics

From the solution of the two-body problem we can express the geocentric right ascension and declination in terms of the orbital element set. Using the symbols defined below, the results are

$$\alpha = \Omega + \tan^{-1}(\text{cositanu}), \quad \delta = \sin^{-1}(\text{sinisinu}) \qquad (1)$$

a = semi-major axis

e = eccentricity

ω = argument of perigee

i = inclination

Ω = longitude of the ascending node

T = time of perigee passage

v = true anomaly

$u = v + \omega$ = argument of latitude

E = eccentric anomaly

M = mean anomaly

n = mean motion

α = geocentric right ascension

δ = geocentric declination

τ = local sidereal time

ϕ' = geocentric latitude of the observer

A = topocentric right ascension

Δ = topocentric declination

Because I have assumed the orbit is circular, $e = 0$. I can now define T and Ω such that $\omega = 0$. Then, at time t,

$$u = v + \omega = v = M = E = n(t - T)$$

Rewrite the expression for the mean anomaly as

$$M = M_Z + n(t - t_Z)$$

where t_Z is the Universal Time corresponding to zenith passage.

As I will explicitly show below, at the zenith,

$$\alpha = A = \tau \text{ and } \delta = \Delta = \phi'$$

for any observer. Thus, since $\alpha = \tau$ and $\delta = \phi'$ at the zenith by definition, it follows that Eqs. (1) implies Eqs. (2);

$$\tau_Z = \Omega + \tan^{-1}(\text{cositan}M_Z), \quad \phi' = \sin^{-1}(\text{sinisin}M_Z) \qquad (2)$$

For our observatory $\phi' > 0$. Hence, as $i \in [0,\pi]$ and $\text{sini} \geq 0$, it follows that $M_Z \in [0,\pi]$ too. Equations (2) are two equations

in three unknowns. The angular velocity provides two more equations and introduces the fourth unknown (i.e., a). Before seeing this I need to project the geocentric motion onto the topocentric celestial sphere.

C. Topocentric Appearance

Let the observer's geocentric location be given by $\underline{\rho} = \rho\underline{\ell}(\tau,\phi')$ where $\underline{\ell}$ is a unit vector of direction cosines in the equatorial coordinate system. The satellite's geocentric location in this reference frame can be written as $\underline{r} = r\underline{\ell}(\alpha,\delta)$. The topocentric location is $\underline{R} = R\underline{\ell}(A,\Delta)$,

$$\underline{R} = \underline{r} - \underline{\rho} \tag{3}$$

Equation (3) can be rewritten in component form as

$$\tan(\alpha - A) = \frac{p\sin h}{1 - p\cos h} \tag{4}$$

$$\tan(\delta - \Delta) = \frac{q\sin(\gamma - \delta)}{1 - q\cos(\gamma - \delta)}$$

$$R/r = \sin(\delta - \gamma)\csc(\Delta - \gamma)$$

where the auxilary quantities p, q, and Υ are defined by

$$p = (\rho/r)\cos\phi'\sec\delta$$

$$q = (\rho/r)\sin\phi'\csc\Upsilon \tag{5}$$

$$\tan\Upsilon = \tan\phi'\cos[(\alpha - A)/2]\sec[h + (\alpha - A)/2]$$

h is the hour angle = $\tau - \alpha$.

Note that h = 0 when $\tau = \alpha$, that is for any object on the celestial meridian there is no parallax in right ascension. Therefore, $\alpha = A$ at the zenith. Note too that if h = 0 and $\alpha = A$ then $\Upsilon = \phi'$. Whence if $\delta = \phi'$ too (i.e., at the astronomical zenith), $\delta = \Delta$ from the middle of Eqs. (4). This proves my assertions earlier.

Differentiate Eq. (3) once with respect to the time t and solve for $\dot{R}$, $\dot{A}$, and $\dot{\Delta}$. Evaluate the results at the zenith [wherein $R = r - \rho$ despite the apparent indeterminateness in the last of Eqs. (4)]. You will find

$$\dot{R}_z = 0, \quad \dot{A}_z = \frac{a\dot{\alpha}_z - \rho\dot{\tau}}{a - \rho}, \quad \dot{\Delta}_z = \frac{a\dot{\delta}_z}{a - \rho} \tag{6}$$

I have replaced r by a because e is zero.

From the differentiated version of Eqs. (1) and the fact

that $u = n(t - T)$ in this instance one finds

$$\dot{\alpha} = \frac{n\cos i \sec^2 M}{1 + \cos^2 i \tan^2 M}, \quad \dot{\delta} = n \sin i \sec\phi' \cos M$$

Now it is known that $M_Z \in [0,\pi]$. So, either M_Z is an acute angle and $\sin M_Z = \sin\phi' \csc i$ or M_Z is an obtuse angle and can be written as $M_Z = \pi - m_Z$ where $m_Z \in [0,\pi/2]$. As in this instance, $\sin M_Z = \sin(\pi - m_Z) = \sin m_Z = \csc i \sin\phi'$, $\tan M_Z = \pm \sin\phi'/(\sin^2 i - \sin^2\phi')^{1/2}$ in the two cases. Only the square of this is needed,

$$\dot{\alpha}_Z = n\cos i \sec^2\phi', \quad \dot{\delta}_Z = n \sin i \sec\phi' \cos M_Z$$

Observe that if M_Z is less than or equal to $\pi/2$ then $\cos M_Z = +(\sin^2 i - \sin^2\phi')^{1/2} \csc i$ whereas if M_Z is greater than or equal to $\pi/2$, $\cos M_Z = -\cos m_Z = -(\sin^2 i - \sin^2\phi')^{1/2} \csc i$. Therefore,

$$\dot{\delta}_Z = \pm\, n(\sin^2 i - \sin^2\phi')^{1/2} \sec\phi' \quad \begin{cases} M_Z \text{ acute} \\ M_Z \text{ obtuse} \end{cases}$$

From Eqs. (6) it follows that the sign of $\dot{\Delta}_Z$ is the same as that as $\dot{\delta}_Z$. Moreover, $\mathrm{sgn}(\dot{\Delta}_Z)$ is a quantity that is determined by the observations themselves. Whence, the correct quadrant for M_Z can be ascertained by observing the north-south direction of motion. Finally, for the topocentric angular velocity,

$$\dot{A}_z = \frac{na\cos i\sec^2\phi' - \rho\dot{\tau}}{a - \rho}, \quad \dot{\Delta}_z = \pm \frac{na(\sin^2 i - \sin^2\phi')^{1/2}\sec\phi'}{a - \rho} \tag{7}$$

Before proceeding to a calculation of the motion as seen projected onto the telescope's focal plane, which is what is recorded by the videotape recorder, consider the topocentric angular speed $\dot{\theta}_z$,

$$\dot{\theta}_z = (\dot{A}_z^2\cos^2\Delta_z + \dot{\Delta}_z^2)^{1/2} \tag{8}$$

$$= \frac{na}{a - \rho}\left[1 - 2(\rho\dot{\tau}/na)\cos i + (\rho\dot{\tau}/na)^2\cos^2\phi'\right]^{1/2}$$

For a polar orbit, and many near-Earth satellites are nearly in such an orbit,

$$\dot{\theta}_z = \frac{na}{a - \rho}\left[1 + (\rho\dot{\tau}/na)^2\cos^2\phi'\right]^{1/2}$$

$$\simeq \frac{na}{a - \rho}\left[1 + \frac{1}{2}(\rho\dot{\tau}/na)^2\cos^2\phi'\right]$$

as $na >> \rho\dot{\tau}$. Thus, the binomial theorem expansion is especially accurate in this case. It should also be clear that for a fixed value of a, $\dot{\theta}_z$ is a maximum for a polar orbit. Table 1 provides a matrix of $\dot{\theta}_z$ values (in deg/sec) for R_z = 100(100) 1500 km and i = 35(10)85, 90°.

TABLE 1

TOPOCENTRIC ANGULAR SPEED (DEG/SEC)

R_z \ i, km	35°	45°	55°	65°	75°	85°	90°
100	4.278	4.309	4.346	4.388	4.432	4.478	4.502
200	2.122	2.138	2.156	2.177	2.199	2.222	2.234
300	1.403	1.414	1.426	1.440	1.455	1.470	1.478
400	1.044	1.052	1.061	1.072	1.083	1.094	1.100
500	0.829	0.835	0.843	0.851	0.860	0.869	0.874
600	0.686	0.691	0.697	0.704	0.711	0.719	0.723
700	0.583	0.588	0.593	0.599	0.605	0.612	0.615
800	0.507	0.511	0.515	0.520	0.526	0.532	0.535
900	0.447	0.451	0.455	0.459	0.464	0.469	0.472
1000	0.399	0.403	0.406	0.410	0.415	0.420	0.422
1100	0.361	0.363	0.367	0.371	0.375	0.379	0.381
1200	0.328	0.331	0.334	0.337	0.341	0.345	0.347
1300	0.301	0.303	0.306	0.309	0.313	0.316	0.318
1400	0.278	0.280	0.282	0.285	0.289	0.292	0.293
1500	0.257	0.259	0.262	0.265	0.268	0.271	0.272

D. Focal Plane Coordinates

The motion we are interested in appears to occur on the surface of a sphere. We analyze it after projection onto the focal plane of the telescope. The nature of this projection is complicated but for small fields of view the results are simple. So, incorporating this new approximation into our analysis, the rectangular coordinates ξ, η in the camera's focal plane (measured in the same units as the telescope's focal length f), where η is positive northward (increasing declination) and ξ is positive eastward (increasing right ascension), are given by

$$\xi/f = (A - A^*)\cos\Delta^*, \quad \eta/f = \Delta - \Delta^* \tag{9}$$

In Eqs. (9) ξ and η are the rectangular coordinates appropriate for an object near the optical axis of the telescope when the object's topocentric right ascension and declination are A, Δ. The topocentric equatorial coordinates of the point where the (extended) optical axis of the telescope would pierce the sky are A^*, Δ^*.

Now, since I have assumed that the field of view is small, it follows that for the cases of interest (n large) the transit time across the field of view will be short. Therefore, a sufficiently accurate representation of A and Δ around the time of zenith passage is just the first two terms in a power series in $t - t_z$;

$$A = A_Z + \dot{A}_Z(t - t_Z), \quad \Delta = \Delta_Z + \dot{\Delta}_Z(t - t_Z)$$

A_Z and Δ_Z are just equal to τ and ϕ'. $\dot{A}_Z$ and $\dot{\Delta}_Z$ were last seen in Eqs. (7). Combining this information with Eqs. (9), and the fact that $A^* = \tau$, $\Delta^* = \phi'$, yields

$$\xi/f = \dot{A}_Z(t - t_Z)\cos\phi', \quad \eta/f = \dot{\Delta}_Z(t - t_Z)$$

The speed of motion across the field of view is $(\dot{\xi}^2 + \dot{\eta}^2)^{1/2}$ which is, it turns out, just $f\dot{\theta}_Z$; $\dot{\theta}_Z$ was given in Eq. (8). The slope of the streak, $d\eta/d\xi$, is

$$s = \frac{d\eta}{d\xi} = \pm \frac{na(\sin^2 i - \sin^2\phi')^{1/2}\sec^2\phi'}{(na\cos i\sec^2\phi' - \rho\dot{\tau})} \tag{10}$$

where the plus or minus sign ambiguity still stems from the quadrant ambiguity for M_Z. Take the limit as $na/\rho\dot{\tau} \to \infty$. Then,

$$\dot{\theta}_Z \to [GM_E/a(a - \rho)^2]^{1/2} \tag{11a}$$

since $n^2a^3 = GM_E$, and

$$s \to \pm (\sin^2 i - \sin^2\phi')^{1/2} \sec i$$

Or, solving for the inclination (s is the slope of the streak determined by the least squares fit referred to earlier)

$$\cos i = \pm \frac{\cos\phi'}{(1 + s^2)^{1/2}} \qquad (11b)$$

Now the plus/minus sign ambiguity is from a square root operation.

In this approximation one can proceed as follows:

1. Note the direction of motion. This fixes the sign of $\dot{\Delta}_Z$ and the quadrant for M_Z.
2. Calculate $f\dot{\theta}_Z$ from the videotapes as discussed in subsection A. Solve the cubic equation for the semi-major axis a in Eq. (11a).
3. Determine the slope of the streak as discussed in subsection A and use it in Eq. (11b). This provides a value for the inclination i. The correct quadrant for i is fixed by the second part of Eqs. (2). Obtain a value for M_Z from this expression too.
4. Use the time of zenith passage plus the first part of Eqs. (2) to calculate the longitude of the ascending node Ω.
5. Refine a and i as necessary from Eqs. (8,10) in an iterative fashion and repeat steps 3, 4, 5.

E. The General Problem

Equations (1) and their derivatives are four equations in the four unknowns a, i, Ω, and T. Projecting them onto the topocentric celestial sphere via Eqs. (4, 5) introduces no new variables. Actually there is a better representation in terms of topocentric variables given by

$$\sin(\alpha - A) = p\sin H$$

$$\sin(\delta - \Delta) = q\sin(\Upsilon - \Delta)$$

where p, q, and Υ are defined in Eqs. (5) and $H = \tau - A$. Finally, the modelling of the motion across the focal plane in Eqs. (9) also introduces no new variables. Thus, ξ, η and their derivatives are connected to a, i, Ω, and T albeit indirectly. Moreover, there appears to be no way to elegantly solve the problem numerically.

III. PARALLAX

A. Data Acquisition

In this instance the near-Earth satellite was so close ($\leq$ 1000 km) to us that we could separately resolve the two streaks from the two telescopes at the ETS after the videotapes were overlaid (see Fig. 3). The distance between corresponding points on the streaks is the parallax. This is related to the topocentric distance of the satellite. Since we are assuming a circular orbit and zenith passage, the topocentric distance is just $a - \rho$ [use L'Hospital's rule on the last of Eqs. (4) for an analytical demonstration of the geometrically obvious]. Therefore, we can compute the semi-major axis a. The inclination of the orbit comes from a measurement of the slope of the streak. Note that since a is smaller for this class of satellites than those treated above, this is an even better approximation.

Looking at Fig. 3 it is imperative to realize that the parallax is the distance between <u>corresponding</u> points on the two streaks and not the perpendicular distance between the two streaks. We now need to consider how to go from the experimental setup to the appropriate quantity.

B. The Geometry

Consider an observer located at $\underline{\rho} = \rho\underline{\ell}(\tau,\phi')$. In detail, this observer has a geocentric distance ρ, a geocentric latitude

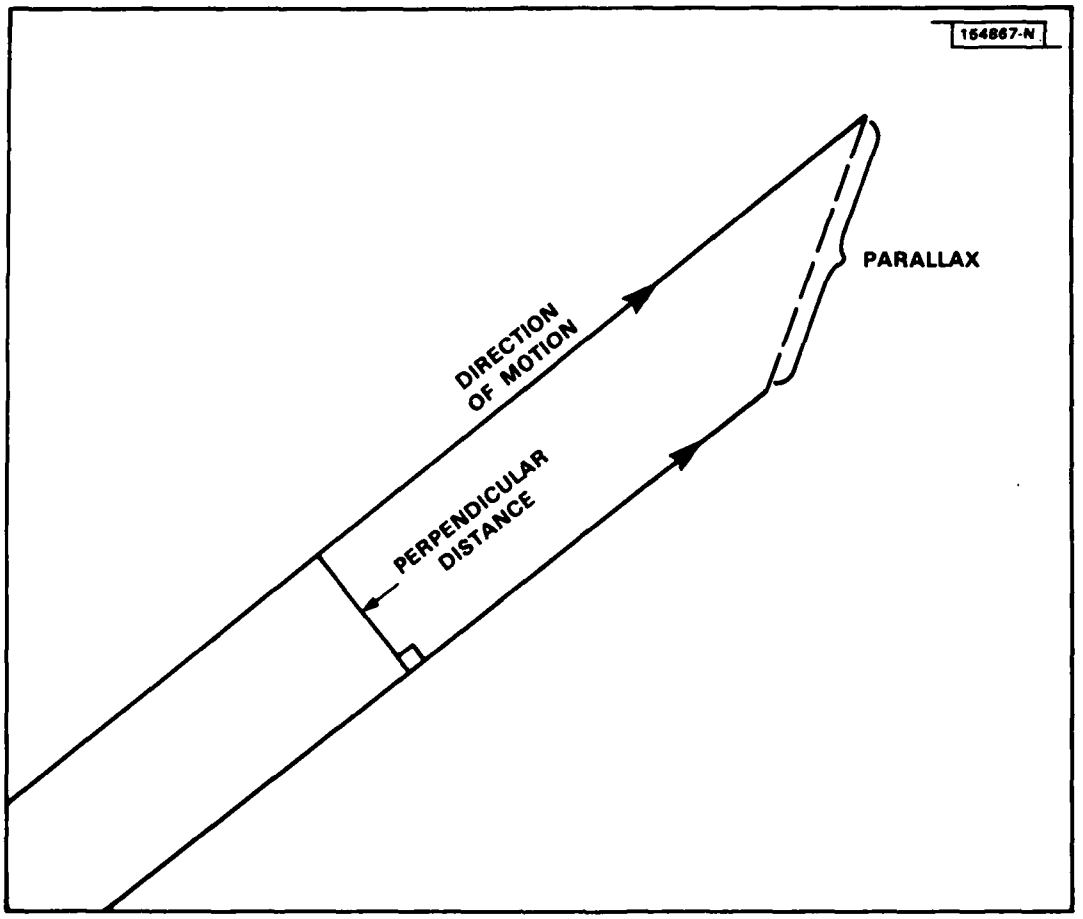

Figure 3. Schematic representation of a pair of simultaneous video frames overlaid. In this case (unlike Fig. 1), the satellite is so close that a parallax can be detected. Note the distinction between the distance between the streaks and the parallax itself. The parallax is the distance between corresponding (i.e., simultaneously occurring) points on the streaks.

ϕ', and a geocentric west longitude λ. The local sidereal time depends upon λ and the Universal Time t via

$$\tau = \text{constant} + 1.0027379093t - \lambda$$

The numerical constant exhibited is just $\dot{\tau}$ in Eq. (6). Let this observer perceive a satellite at topocentric position A and Δ when it has geocentric location $\underline{r} = r\underline{\ell}(\alpha,\delta)$. Equations (3, 4, and 5) provide the interrelationships.

Now consider a second, nearby observer whose geocentric location is given by $\rho + \Delta\rho$, $\phi' + \Delta\phi'$, and $\lambda + \Delta\lambda$. At the same instant of time he will perceive the satellite to be at $A + \Delta A$ and $\Delta + \Delta\Delta$ where

$$\tan(\alpha - A - \Delta A) = \frac{(p + \Delta p)\sin(h + \Delta h)}{1 - (p + \Delta p)\cos(h + \Delta h)}$$

$$\tan(\delta - \Delta - \Delta\Delta) = \frac{(q + \Delta q)\sin(\Upsilon + \Delta\Upsilon - \delta)}{1 - (q + \Delta q)\cos(\Upsilon + \Delta\Upsilon - \delta)}$$

Although written in a suggestive form, these equations are exact. If $|\Delta\rho|$ and $\rho[(\Delta\lambda\cos\phi')^2 + (\Delta\phi')^2]^{1/2}$ are both small quantities compared to ρ, then we may simplify these results, for ΔA, $\Delta\Delta$, Δp, Δq, and $\Delta\Upsilon$ will all be small in magnitude too. Summarizing several pages of algebra,

$$\Delta A = \frac{p\Delta\lambda\cosh - \Delta p\sinh - p^2\Delta\lambda}{1 - 2p\cosh + p^2}$$

$$\Delta\Delta = \frac{-q\Delta\gamma\cos(\gamma - \delta) - \Delta q\sin(\gamma - \delta) + q^2\Delta\gamma}{1 - 2q\cos(\gamma - \delta) + q^2} \qquad (12)$$

$$\Delta\gamma\sec\gamma\csc\gamma = (\Delta A/2)\{\tan[(\alpha - A)/2] - \tan[h + (\alpha - A)/2]\} +$$
$$\Delta\phi'\sec\phi'\csc\phi' - \Delta\lambda\tan[h + (\alpha - A)/2]$$

$$\Delta p/p = \Delta\rho/\rho - \Delta\phi'\tan\phi'$$
$$\Delta q/q = \Delta\rho/\rho + \Delta\phi'\cot\phi' - \Delta\gamma\cot\gamma$$

and, since $\Delta h = -\Delta\lambda$

$$\Delta R/R = [\cot(\Delta - \gamma) - \cot(\delta - \gamma)]\Delta\gamma - \Delta\Delta\cot(\Delta - \gamma)$$

C. Focal Plane Formulas

Once again each observer records the events as projected onto his focal plane. If they both have small fields of view, then the approximation in Eqs. (9) is appropriate. If the first observer measures ξ, η corresponding to A, Δ, then the second one will obtain $\xi + \Delta\xi$ and $\eta + \Delta\eta$ corresponding to $A + \Delta A$ and $\Delta + \Delta\Delta$. As $\Delta A^* = -\Delta\lambda$ and $\Delta\Delta^* = \Delta\phi'$,

$$\Delta\xi/f = -(A - A^*)\Delta\phi'\sin\Delta^* + (\Delta A + \Delta\lambda)\cos\Delta^* \qquad (13a)$$

$$\Delta\eta/f \simeq \Delta\Delta - \Delta\phi' \tag{13b}$$

The separation between corresponding points on the streaks is equal to $[(\Delta\xi)^2 + (\Delta\eta)^2]^{1/2}$.

However, all of this occurs near a zenith passage. Thus, $h \simeq 0$, $\alpha \simeq A \simeq A^* = \tau$, $\delta \simeq \Delta \simeq \Delta^* = \phi'$, $\Upsilon = \phi'$, and $p \simeq q \simeq \rho/r = \rho/a$. From Eqs. (12),

$$\Delta A \rightarrow \frac{p\Delta\lambda}{1 - p}, \quad \Delta\Delta \rightarrow \frac{-q\Delta\Upsilon}{1 - q}, \text{ and } \Delta\Upsilon \rightarrow \Delta\phi'$$

Therefore, Eqs. (13) may be approximately written as

$$\Delta\xi/f = \frac{\Delta\lambda\cos\phi'}{1 - \rho/a}, \quad \Delta\eta/f = \frac{-\Delta\phi'}{1 - \rho/a} \tag{14}$$

The distance between corresponding points on the streak is

$$\frac{[(\Delta\lambda\cos\phi')^2 + (\Delta\phi')^2]^{1/2}}{1 - \rho/a}$$

Were this measured we could compute the semi-major axis a for a known observer separation.

D. Data Analysis - Two Parallel Lines

If all one has is two parallel streaks, near the center of the field of view, from two telescopes pointing nearly

zenithally, then one can no longer determine which are corresponding pairs of points. The reason is simple - we are looking at a static picture wherein all time information concerning the development of the streaks has been lost. Hence, we must proceed in another fashion.

Let (ξ_1,η_1) be the values of ξ, η at time t_1 for the first observer. The corresponding values of these coordinates for the second observer will be $(\xi_1 + \Delta\xi,\eta_1 + \Delta\eta)$. At time t_2 the first observer measures (ξ_2,η_2). For the corresponding point on his streak the second observer will deduce $(\xi_2 + \Delta\xi,\eta_2 + \Delta\eta)$. Note that there is no time dependence in $\Delta\eta$ or $\Delta\xi$, see Eqs. (14). That is why the corresponding points are identically offset and, therefore, why the two streaks are parallel.

Use the two-point form of the equation of a straight line to deduce the equations for the two streaks. Then recast the result in the slope-intercept form. The results are

$$\eta = m\xi + b, \quad m = \frac{\eta_2 - \eta_1}{\xi_2 - \xi_1}, \quad b = \frac{\xi_2\eta_1 - \xi_1\eta_2}{\xi_2 - \xi_1}$$

$$\eta = m\xi + B, \quad B = b + \Delta\eta - m\Delta\xi \tag{15}$$

The two slopes are the same but the y-intercepts are different. Clearly if we can determine b, B, and m, then in light of Eqs. (14), we can determine the semi-major axis a.

As our instruments and measuring devices are not perfect, we do not measure ξ, η but approximations to them, say x, y. Suppose that we make N measurements on the fainter streak $\{(x_n,y_n)\}$ and N measurements on the brighter streak $\{(X_n,Y_n)\}$. Then, since it is more difficult to measure fainter streaks than it is to measure brighter ones, we weight the measures on the fainter streak by $w \in [0,1]$. A logical sum of the squares of the residuals to consider is

$$S = \sum_{n=1}^{N} \{w[y_n - (mx_n + b)]^2 + [Y_n - (mX_n + B)]^2\}$$

Minimizing S with respect to m, b, and B provides three normal equations for their determination. From these values and the knowledge of ρ, $\Delta\phi'$, and $\Delta\lambda$ comes a if the relationship (15) is utilized.

With a and i determined and the direction of motion known, Eqs. (2) yields M_z and then Ω since we know the time of observation.

E. The Inclination

There is a purely geometric way to deduce the inclination. One need only draw the topocentric celestial sphere and reflect upon the four exhaustive and exclusive possibilities shown in Fig. 4. By solving the node, zenith, and meridian/equator intersection right spherical triangle, one comes to Eq. (11b).

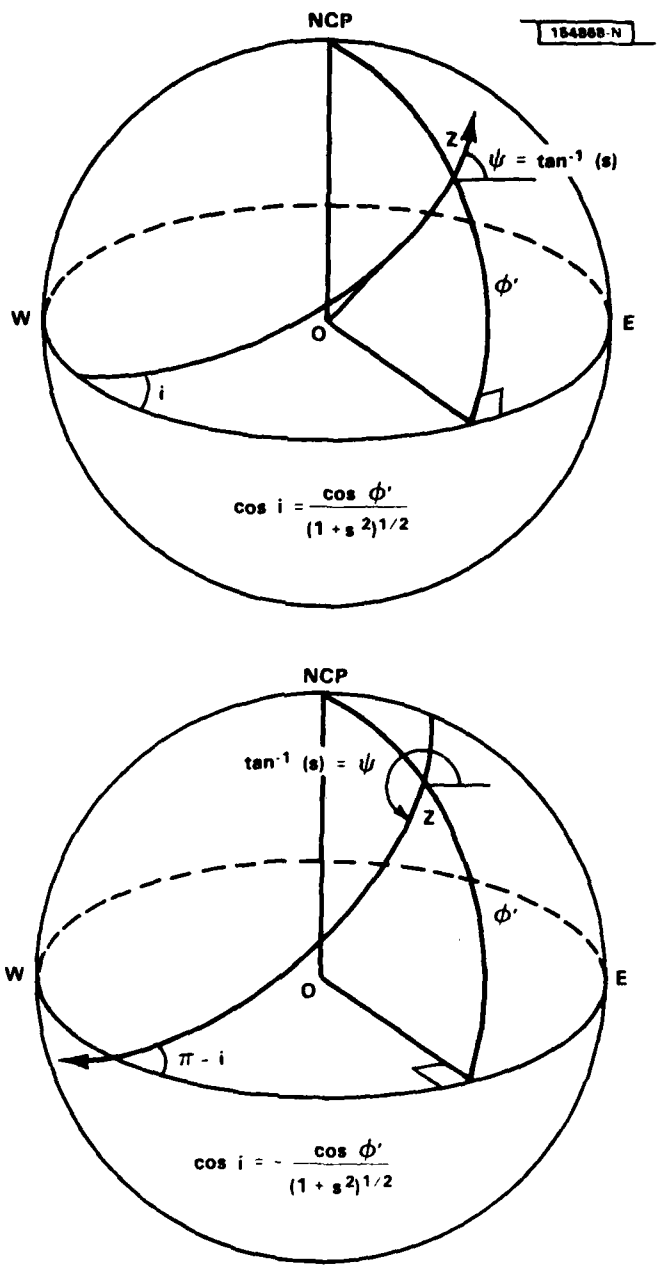

Figure 4. Spherical triangles for the four exhaustive and mutually exclusive kinds of zenith passage.

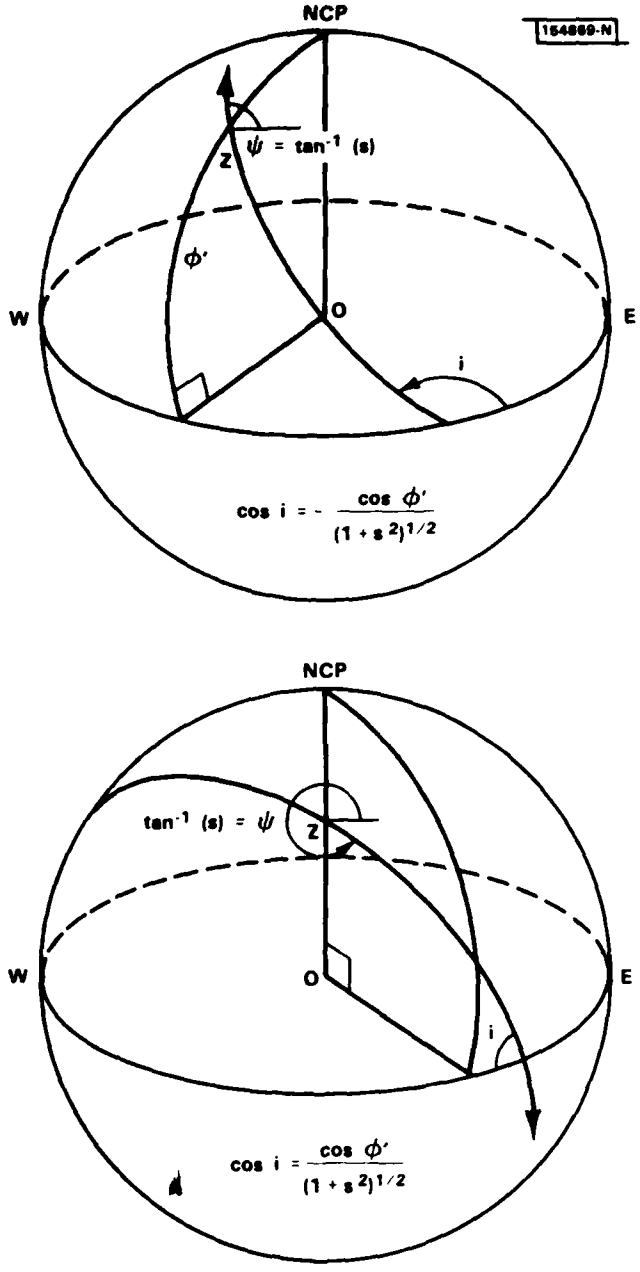

Figure 4. (Continued)

UNCLASSIFIED

SECURITY CLASSIFICATION OF THIS PAGE *(When Data Entered)*

REPORT DOCUMENTATION PAGE		READ INSTRUCTIONS BEFORE COMPLETING FORM
1. REPORT NUMBER ESD-TR-85-263	2. GOVT ACCESSION NO.	3. RECIPIENT'S CATALOG NUMBER
4. TITLE *(and Subtitle)* The Analysis of Near-Earth Satellite Astrometric Data at the ETS		5. TYPE OF REPORT & PERIOD COVERED Project Report 6. PERFORMING ORG. REPORT NUMBER Project Report ETS-76
7. AUTHOR(s) Laurence G. Taff		8. CONTRACT OR GRANT NUMBER(s) F19628-85-C-0002
9. PERFORMING ORGANIZATION NAME AND ADDRESS Lincoln Laboratory, M.I.T. P.O. Box 73 Lexington, MA 02173-0073		10. PROGRAM ELEMENT, PROJECT, TASK AREA & WORK UNIT NUMBERS Program Element Nos. 63428F and 1242F Project Nos. 2698 and 2295
11. CONTROLLING OFFICE NAME AND ADDRESS Air Force Command, USAF Andrews AFB Washington, DC 20331		12. REPORT DATE 12 December 1985 13. NUMBER OF PAGES 34
14. MONITORING AGENCY NAME & ADDRESS *(if different from Controlling Office)* Electronic Systems Division Hanscom AFB, MA 01731		15. SECURITY CLASS. *(of this Report)* Unclassified 15a. DECLASSIFICATION DOWNGRADING SCHEDULE

16. DISTRIBUTION STATEMENT *(of this Report)*

Approved for public release; distribution unlimited.

17. DISTRIBUTION STATEMENT *(of the abstract entered in Block 20, if different from Report)*

18. SUPPLEMENTARY NOTES

None

19. KEY WORDS *(Continue on reverse side if necessary and identify by block number)*

angles-only data
parallax
near-earth satellite
orbital element sets
celestial mechanics
data reduction
zenithal observations

20. ABSTRACT *(Continue on reverse side if necessary and identify by block number)*

The activities at the ETS have expanded from observations of deep-space artificial satellites during the dark hours to observations of near-Earth satellites near noon. Not only do these varying tasks require different video cameras and associated equipment, they can benefit from a tailored analysis of the resulting astrometric data. In particular, the observation of near-Earth artificial satellites very near the astronomial zenith has become a frequent mode of operation. For some of these satellites a parallax can be discerned when both ETS telescopes are used. For others, their nearly circular orbit coupled with a zenith passage suffices to fix their element set. This Project Report details both types of analysis.

DD FORM 1 Jan 73 1473 EDITION OF 1 NOV 65 IS OBSOLETE

UNCLASSIFIED

SECURITY CLASSIFICATION OF THIS PAGE *(When Data Entered)*

END

FILMED

3-86

DTIC